

## DERIVING ANALYTICAL SOLUTIONS FOR THE FRACTIONAL BURGERS-HUXLEY (FBH) EQUATION: THE ROLE OF THE TANH-COTH METHOD

*Ali Satty, Abaker A. Hassaballa, Mohyaldein Salih, Mnahil Bashier, Elzain A.E. Gumma*

*Department of Mathematics, College of Science, Northern Border University, Arar, Saud Arabia  
alisatty1981@gmail.com, abakerh@gmail.com, mohyyassin@gmail.com  
munahilbashier@yahoo.com, elzain.elzain@gmail.com*

Received: 20 September 2024; Accepted: 26 February 2025

**Abstract.** This paper focuses on the nonlinear Fractional Burgers-Huxley (FBH) equation in space-time, using the conformable fractional derivative (CFD) method. The paper aims to investigate the application of the Tanh-Coth method in order to find exact solutions to the FBH equation. Various exact analytical solutions for the FBH equation are obtained. Graphical representations are included to show the physical properties of the obtained solutions. The results reveal that the Tanh-Coth method is effective and dependable for finding exact solutions to the nonlinear FBH equation.

**MSC 2010:** 35C07, 35C08

**Keywords:** *fractional Burgers-Huxley (FBH) equation, Tanh-Coth method, nonlinear partial differential equation, conformable fractional derivative (CFD)*

### 1. Introduction

Nonlinear partial differential equations (NPDEs) are fundamental in characterizing complex systems across different scientific areas. NPDEs are essential for illustrating the intricacies of nonlinear phenomena, such as wave propagation and pattern formation, areas where linear models cannot be characterized. Acquiring exact analytical solutions for NPDEs is crucial for gaining a deeper insight into the complex behaviors provided in various disciplines like fluid dynamics [1], plasma physics [2], and biological systems [3]. Recently, studies have developed several advanced numerical methods for solving NPDEs, providing robust tools to estimate solutions when analytical approaches are inadequate [4-6]. Approaches like the Tanh-Coth method, Adomian decomposition method, variational iteration method, and Bernoulli sub-equation function have demonstrated great potential to solve NPDEs with impressive accuracy and efficiency [7-10]. By improving the ability to address intricate

nonlinear problems, these approaches also extend the range of applications in today's scientific research [7, 11].

As given in [12], the general form of the Burgers-Huxley equation (BHE) can be mathematically shown as follows:

$$u_t - u_{xx} + \beta uu_x - \gamma u(\lambda - u^\tau)(u^\tau - 1) = 0. \quad (1)$$

In this equation,  $u(x, t)$  represents a function dependent on both the spatial variable ( $x$ ) and the temporal variable ( $t$ ), with  $\lambda$ ,  $\tau$ ,  $\gamma$  and  $\beta$  being constants. When  $\tau = 1$  and  $\beta = 0$ , equation (1) reduces to the Huxley equation, which elucidates the dynamics of wall motion in liquid crystals and the propagation of nerve impulses in neural fibers:  $u_t - u_{xx} - \gamma u(\lambda - u)(u - 1) = 0$ . Similarly, when  $\tau = 1$  and  $\gamma = 0$ , equation (1) simplifies to the Burgers' equation, which models the far field of wave propagation in nonlinear dissipative systems:  $u_t - u_{xx} + \beta uu_x = 0$ . For  $\tau = 1$  and  $\beta \neq 0, \gamma \neq 0$ , equation (1) transforms into the BHE:  $u_t - u_{xx} + \beta uu_x - \gamma u(\lambda - u)(u - 1) = 0$ . When  $\beta = -1, \gamma = 1$  and  $\tau = 1$ , equation (1) transforms into a BHE as described in [13]:

$$u_t - u_{xx} - uu_x - u(\lambda - u)(u - 1) = 0. \quad (2)$$

The Fractional BHE (FBHE) in space-time is mathematically presented as:

$$D_t^\alpha u - D_x^{\alpha\alpha} u - u D_x^\alpha u - u(\lambda - u)(u - 1) = 0. \quad (3)$$

This equation integrates the Burgers' and Huxley equations with fractional calculus, enabling the modeling of complex systems and effectively capturing phenomena such as anomalous diffusion, memory effects, and non-local correlations. The equation is employed in various applications like material science, biology and fluid dynamics for modeling viscoelastic materials, studying anomalous diffusion and characterizing nonlinear wave propagation and turbulence, respectively. Within the use of fractional derivatives, the equation effectively captures systems characterized by memory and nonlocal interactions, enhancing the accuracy of modeling complicated real-world phenomena. This study demonstrates exact wave solutions of this equation by employing the conformable fractional derivative (CFD) [14]. CFD, an advanced tool in fractional calculus, gives a more intuitive and physically meaningful interpretation, allowing for the modeling of systems that exhibit memory effects and non-local interactions, where changes are influenced by the current state and the history of the system. CFD retains essential properties such as linearity, the product rule, and the chain rule, showing a versatile framework for capturing complex, real-world phenomena. By applying these properties, this study illustrates CFD's effectiveness in solving the FBHE in space-time, thereby enhancing the fields of fractional calculus, and nonlinear dynamics. In equation (3), the CFD denotes time  $t$  and space  $x$  as  $D_t^\alpha$  and  $D_x^\alpha$  respectively. Higher-order derivatives are defined as  $D_x^{\alpha\alpha} u = D_x^\alpha(D_x^\alpha u)$  for second-order. In terms of independent variables, the CFD is defined by an order  $\alpha$  ( $0 < \alpha \leq 1$ ) and can be mathematically expressed as:

$$D^\alpha u(s) = \lim_{\tau \rightarrow 0} \frac{u(s+\tau s^{1-\alpha}) - u(s)}{\varepsilon \tau} \quad \forall t > 0, \alpha \in (0,1].$$

$$u^{(\alpha)}(0) = \lim_{s \rightarrow 0^+} u^{(\alpha)}(s).$$

When  $\alpha$  equals 1 in the previous equations, the non-integer differential changes to the commonly known integer differential. Further explanations of CFD can be found in [14]. Taking advantage of CFD properties, this study employs the Tanh-Coth method [15] to acquire exact wave solutions for equation (3). This method is used in this study due to its efficiency in addressing nonlinear differential equations, providing advantages such as creating various solution forms and ease of implementation. The method is also effective for NLPDEs with particular structural properties, particularly those transformable into hyperbolic functions. Yet, it falters with equations that have chaotic, irregular, or complex boundary conditions and lack symmetry or integrability. This study extends the emphasis on the focus on fractional dimensions, with respect to the FBHE, as demonstrated by references [16-19].

In contrast to prior studies (see [20-25]) that have extensively employed the Tanh-Coth method to various NPDEs, this study uniquely focuses on its application, a context in which this method has yet to be explored. The originality of this study arises from applying the Tanh-Coth method specifically for the FBHE, particularly filling a gap in its application to this equation. The main objective is to apply the Tanh-Coth method to derive exact solutions for the FBHE for various fractional order conditions. The motivation of this study comes from the need to create efficient and reliable methods for solving NPDEs, indispensable for modeling real-world phenomena with nonlinear characteristics. A range of exact analytical solutions for the FBHE has been acquired. Visual depictions are presented to elucidate the physical properties of the acquired solutions, illustrating the influence of fractional order. This paper is structured as follows: Section 1 gives the introduction of the study, Section 2 presents the steps of employing the Tanh-Coth method, Section 3 provides the application of the Tanh-Coth method, Section 4 outlines the physical properties and graphs of FBHE solutions, and Section 5 summarizes the results.

## 2. Steps of employing the Tanh-Coth method

As stated in [26], this Tanh-Coth method posits that traveling wave solutions can be visualized through the tanh function, involving the following key steps:

**Step 1:** Consider the following NDPE

$$P(u, D_t^\alpha u, D_x^\alpha u, D_t^{\alpha\alpha} u, D_t^\alpha(D_x^\alpha u), D_x^{\alpha\alpha} u, \dots) = 0, \quad (4)$$

where  $u(x, t)$  is a function that depends on  $x$  and  $t$ .

**Step 2:** To derive solutions for equation (4), the traveling wave transformation is utilized. By setting  $u(x, t) = u(\xi)$  with  $\xi = (x^\alpha - vt^\alpha)/\alpha$ , this transformation converts equation (4) into ordinary differential equation (ODE)

$$Q(u, u', u'', u''', \dots) = 0, \quad (5)$$

where the prime symbol (') represents differentiation with respect to  $\xi$ .

**Step 3:** Introduce a new independent variable

$$X = \tanh(\mu\xi), \quad (6)$$

where  $\mu$  is wave number, which leads to the following transformations of the derivative

$$\begin{aligned} \frac{d}{d\xi} &= \mu(1 - X^2) \frac{d}{dX}, \\ \frac{d^2}{d\xi^2} &= -2\mu^2(1 - X^2) \frac{d}{dX} + \mu^2(1 - X^2)^2 \frac{d^2}{dX^2}, \\ \frac{d^3}{d\xi^3} &= -2\mu^3(1 - X^2)(3X^2 - 1) \frac{d}{dX} - 6\mu^3(1 - X^2)^2 \frac{d^2}{dX^2} + \mu^3(1 - X^2)^3 \frac{d^3}{dX^3}. \\ &\vdots \end{aligned} \quad (7)$$

Other derivatives can be derived in a similar manner.

**Step 4:** Propose an expansion for  $u(x, t)$  as follows

$$u(x, t) = S(X) = \sum_{k=0}^m \rho_k X^k + \sum_{k=1}^m \rho_{-k} X^{-k}, \quad (8)$$

where  $m$  is typically a positive integer. To ascertain the value of  $m$ , the highest order linear terms in equation (5) are typically balanced with the highest order nonlinear terms.

**Step 5:** Once  $m$  is determined, we substitute equation (8) into (5). This substitution transforms the ODE into an equation expressed in powers of  $X$ . We then gather all coefficients of the powers of  $X$  in the resulting equation, ensuring that these coefficients must vanish. This process yields a system of algebraic equations involving the parameters  $\rho_k$  ( $k = 0, \pm 1, \pm 2, \dots, m$ ),  $\mu$  and  $\nu$ . By solving for these parameters and employing equation (8), we can derive an analytic solution  $u(x, t)$  for the FBH equation.

### 3. Utilization of the Tanh-Coth method

The Tanh-Coth method is utilized to derive wave solutions for equation (3). Now, consider the traveling wave transformation as follows:

$$u(x, t) = u(\xi), \quad \xi = \frac{1}{\alpha}(x^\alpha - \nu t^\alpha). \quad (9)$$

Substituting Eq. (9) into Eq. (3) transforms Eq. (3) into an ODE,

$$\nu u' + uu' + u'' + u(\lambda - u)(u - 1) = 0. \quad (10)$$

By setting the nonlinear term  $u^3$  equal to the highest order derivative ( $u''$ ), we determine that  $m = 1$ . As a result,

$$u(\xi) = \rho_{-1}X^{-1} + \rho_0 + \rho_1X. \quad (11)$$

Replacing Eq. (11) in Eq. (10), we get

$$\begin{aligned} & c(\rho_{-1}X^{-1} + \rho_0 + \rho_1X)' + (\rho_{-1}X^{-1} + \rho_0 + \rho_1X)(\rho_{-1}X^{-1} + \rho_0 + \rho_1X)' \\ & + (\rho_{-1}X^{-1} + \rho_0 + \rho_1X)'' + (\rho_{-1}X^{-1} + \rho_0 + \rho_1X) \\ & \times (\lambda - (\rho_{-1}X^{-1} + \rho_0 + \rho_1X))((\rho_{-1}X^{-1} + \rho_0 + \rho_1X) - 1) = 0. \end{aligned} \quad (12)$$

By substituting equation (12) back into equation (10) and systematically organizing all terms according to their respective powers of  $X$ , we derive a set of algebraic equations by setting each term's coefficient to zero in equation (10). These resulting algebraic equations are subsequently solved using Maple's computational tools to produce the following solution sets.

**Case 1:** Upon investigation, in case of  $\rho_{-1} = 0$ , we get

$$\rho_0 = \frac{1}{2}, \rho_1 = \frac{1}{2}, \mu = \frac{1}{2}, \nu = \lambda - 1. \quad (13)$$

$$\rho_0 = \frac{1}{2}, \rho_1 = -\frac{1}{2}, \mu = -\frac{1}{2}, \nu = \lambda - 1. \quad (14)$$

$$\rho_0 = \frac{1}{2}\lambda, \rho_1 = \frac{1}{2}\lambda, \mu = \frac{1}{2}\lambda, \nu = 1 - \lambda. \quad (15)$$

$$\rho_0 = \frac{1}{2}\lambda, \rho_1 = -\frac{1}{2}\lambda, \mu = -\frac{1}{2}\lambda, \nu = 1 - \lambda. \quad (16)$$

$$\rho_0 = \frac{1}{2}\lambda + \frac{1}{2}, \rho_1 = -\frac{1}{2}\lambda + \frac{1}{2}, \mu = -\frac{1}{2}\lambda + \frac{1}{2}, \nu = -(1 + \lambda). \quad (17)$$

$$\rho_0 = \frac{1}{2}\lambda + \frac{1}{2}, \rho_1 = \frac{1}{2}\lambda - \frac{1}{2}, \mu = \frac{1}{2}\lambda - \frac{1}{2}, \nu = -(1 + \lambda). \quad (18)$$

$$\rho_0 = \frac{1}{2}, \rho_1 = \frac{1}{2}, \mu = -\frac{1}{4}, \nu = \frac{1}{2} - 2\lambda. \quad (19)$$

$$\rho_0 = \frac{1}{2}, \rho_1 = -\frac{1}{2}, \mu = \frac{1}{4}, \nu = \frac{1}{2} - 2\lambda. \quad (20)$$

$$\rho_0 = \frac{1}{2}\lambda, \rho_1 = \frac{1}{2}\lambda, \mu = -\frac{1}{4}\lambda, \nu = \frac{1}{2}\lambda - 2. \quad (21)$$

$$\rho_0 = \frac{1}{2}\lambda, \rho_1 = -\frac{1}{2}\lambda, \mu = \frac{1}{4}\lambda, \nu = \frac{1}{2}\lambda - 2. \quad (22)$$

$$\rho_0 = \frac{1}{2}\lambda + \frac{1}{2}, \rho_1 = -\frac{1}{2}\lambda + \frac{1}{2}, \mu = \frac{1}{4}\lambda - \frac{1}{4}, \nu = \frac{1}{2}\lambda + \frac{1}{2}. \quad (23)$$

$$\rho_0 = \frac{1}{2}\lambda + \frac{1}{2}, \rho_1 = \frac{1}{2}\lambda - \frac{1}{2}, \mu = -\frac{1}{4}\lambda + \frac{1}{4}, \nu = \frac{1}{2}\lambda + \frac{1}{2}. \quad (24)$$

**Case 2:** Upon investigation, in case of  $\rho_1 = 0$ , we have

$$\rho_0 = \frac{1}{2}, \rho_{-1} = -\frac{1}{2}, \mu = \frac{1}{4}, \nu = \frac{1}{2} - 2\lambda. \quad (25)$$

$$\rho_0 = \frac{1}{2}, \rho_{-1} = \frac{1}{2}, \mu = \frac{1}{2}, \nu = \lambda - 1. \quad (26)$$

$$\rho_0 = \frac{1}{2}\lambda, \rho_{-1} = -\frac{1}{2}\lambda, \mu = \frac{1}{4}\lambda, \nu = \frac{1}{2}\lambda - 2. \quad (27)$$

$$\rho_0 = \frac{1}{2}\lambda, \rho_{-1} = \frac{1}{2}\lambda, \mu = \frac{1}{2}\lambda, \nu = 1 - \lambda. \quad (28)$$

$$\rho_0 = \frac{1}{2}, \rho_{-1} = \frac{1}{2}, \mu = -\frac{1}{4}, \nu = \frac{1}{2} - 2\lambda. \quad (29)$$

$$\rho_0 = \frac{1}{2}, \rho_{-1} = -\frac{1}{2}, \mu = -\frac{1}{2}, \nu = \lambda - 1. \quad (30)$$

$$\rho_0 = \frac{1}{2}\lambda, \rho_{-1} = \frac{1}{2}\lambda, \mu = -\frac{1}{4}\lambda, \nu = \frac{1}{2}\lambda - 2. \quad (31)$$

$$\rho_0 = \frac{1}{2}\lambda, \rho_{-1} = -\frac{1}{2}\lambda, \mu = -\frac{1}{2}\lambda, \nu = 1 - \lambda. \quad (32)$$

$$\rho_0 = \frac{1}{2}\lambda + \frac{1}{2}, \rho_{-1} = \frac{1}{2}\lambda - \frac{1}{2}, \mu = -\frac{1}{4}\lambda + \frac{1}{4}, \nu = \frac{1}{2}\lambda + \frac{1}{2}. \quad (33)$$

$$\rho_0 = \frac{1}{2}\lambda + \frac{1}{2}, \rho_{-1} = -\frac{1}{2}\lambda + \frac{1}{2}, \mu = -\frac{1}{2}\lambda + \frac{1}{2}, \nu = -(\lambda + 1). \quad (34)$$

$$\rho_0 = \frac{1}{2}\lambda + \frac{1}{2}, \rho_{-1} = -\frac{1}{2}\lambda + \frac{1}{2}, \mu = \frac{1}{4}\lambda - \frac{1}{4}, \nu = \frac{1}{2}\lambda + \frac{1}{2}. \quad (35)$$

$$\rho_0 = \frac{1}{2}\lambda + \frac{1}{2}, \rho_{-1} = \frac{1}{2}\lambda - \frac{1}{2}, \mu = \frac{1}{2}\lambda - \frac{1}{2}, \nu = -(\lambda + 1). \quad (36)$$

**Case 3:** In case where  $\rho_1 \neq 0$  and  $\rho_{-1} \neq 0$ , it is observed that

$$\rho_0 = \frac{1}{2}, \rho_1 = -\frac{1}{4}, \rho_{-1} = -\frac{1}{4}, \mu = \frac{1}{8}, \nu = \frac{1}{2} - 2\lambda. \quad (37)$$

$$\rho_0 = \frac{1}{2}, \rho_1 = \frac{1}{4}, \rho_{-1} = \frac{1}{4}, \mu = -\frac{1}{8}, \nu = \frac{1}{2} - 2\lambda. \quad (38)$$

$$\rho_0 = \frac{1}{2}, \rho_1 = \frac{1}{4}, \rho_{-1} = \frac{1}{4}, \mu = \frac{1}{4}, \nu = \lambda - 1. \quad (39)$$

$$\rho_0 = \frac{1}{2}, \rho_1 = -\frac{1}{4}, \rho_{-1} = -\frac{1}{4}, \mu = -\frac{1}{4}, \nu = \lambda - 1. \quad (40)$$

$$\rho_0 = \frac{1}{2}\lambda, \rho_1 = -\frac{1}{4}\lambda, \rho_{-1} = -\frac{1}{4}\lambda, \mu = \frac{1}{8}\lambda, \nu = \frac{1}{2}\lambda - 2. \quad (41)$$

$$\rho_0 = \frac{1}{2}\lambda, \rho_1 = \frac{1}{4}\lambda, \rho_{-1} = \frac{1}{4}\lambda, \mu = -\frac{1}{8}\lambda, \nu = \frac{1}{2}\lambda - 2. \quad (42)$$

$$\rho_0 = \frac{1}{2}\lambda, \rho_1 = \frac{1}{4}\lambda, \rho_{-1} = \frac{1}{4}\lambda, \mu = \frac{1}{4}\lambda, \nu = 1 - \lambda. \quad (43)$$

$$\rho_0 = \frac{1}{2}\lambda, \rho_1 = -\frac{1}{4}\lambda, \rho_{-1} = -\frac{1}{4}\lambda, \mu = -\frac{1}{4}\lambda, \nu = 1 - \lambda. \quad (44)$$

$$\rho_0 = \frac{1}{2}\lambda + \frac{1}{2}, \rho_1 = \frac{1}{4}\lambda - \frac{1}{4}, \rho_{-1} = \frac{1}{4}\lambda - \frac{1}{4}, \mu = -\frac{1}{8}\lambda + \frac{1}{8}, \nu = \frac{1}{2}\lambda + \frac{1}{2}. \quad (45)$$

$$\rho_0 = \frac{1}{2}\lambda + \frac{1}{2}, \rho_1 = -\frac{1}{4}\lambda + \frac{1}{4}, \rho_{-1} = -\frac{1}{4}\lambda + \frac{1}{4}, \mu = \frac{1}{8}\lambda - \frac{1}{8}, \nu = \frac{1}{2}\lambda + \frac{1}{2}. \quad (46)$$

$$\rho_0 = \frac{1}{2}\lambda + \frac{1}{2}, \rho = -\frac{1}{4}\lambda + \frac{1}{4}, \rho_{-1} = -\frac{1}{4}\lambda + \frac{1}{4}, \mu = -\frac{1}{4}\lambda + \frac{1}{4}, \nu = -(\lambda + 1). \quad (47)$$

$$\rho_0 = \frac{1}{2}\lambda + \frac{1}{2}, \rho = \frac{1}{4}\lambda - \frac{1}{4}, \rho_{-1} = \frac{1}{4}\lambda - \frac{1}{4}, \mu = \frac{1}{4}\lambda - \frac{1}{4}, \nu = -(\lambda + 1). \quad (48)$$

Equations (13) through (24) provide sets of soliton solutions. Such solutions are given by:

$$u_1(x, t) = \frac{1}{2} \left[ 1 + \tanh \left( \frac{1}{2\alpha} (x^\alpha + (\lambda - 1)t^\alpha) \right) \right]. \quad (49)$$

$$u_2(x, t) = \frac{1}{2} \lambda \left[ 1 + \tanh \left( \frac{\lambda}{2\alpha} (x^\alpha + (1 - \lambda)t^\alpha) \right) \right]. \quad (50)$$

$$u_3(x, t) = \frac{1}{2} \left[ (\lambda + 1) + (\lambda - 1) \tanh \left( \frac{1}{2\alpha} (\lambda - 1)(x^\alpha - (1 + \lambda)t^\alpha) \right) \right]. \quad (51)$$

$$u_4(x, t) = \frac{1}{2} \left[ 1 - \tanh \left( \frac{\lambda}{4\alpha} \left( x^\alpha + \left( \frac{1}{2} - 2\lambda \right) t^\alpha \right) \right) \right]. \quad (52)$$

$$u_5(x, t) = \frac{1}{2} \lambda \left[ 1 - \tanh \left( \frac{\lambda}{4\alpha} \left( x^\alpha + \left( \frac{1}{2} \lambda - 2 \right) t^\alpha \right) \right) \right]. \quad (53)$$

$$u_6(x, t) = \frac{1}{2} \left[ (\lambda + 1) - (\lambda - 1) \tanh \left( \frac{1}{4\alpha} (\lambda - 1) \left( x^\alpha + \frac{1}{2} (\lambda + 1) t^\alpha \right) \right) \right]. \quad (54)$$

Also, equations (25) through (36) yield sets of traveling wave solutions:

$$u_7(x, t) = \frac{1}{2} \left[ 1 - \coth \left( \frac{1}{4\alpha} \left( x^\alpha + \left( \frac{1}{2} - 2\lambda \right) t^\alpha \right) \right) \right]. \quad (55)$$

$$u_8(x, t) = \frac{1}{2} \left[ 1 + \coth \left( \frac{1}{2\alpha} (x^\alpha + (\lambda - 1)t^\alpha) \right) \right]. \quad (56)$$

$$u_9(x, t) = \frac{1}{2} \lambda \left[ 1 - \coth \left( \frac{1}{4\alpha} \lambda \left( x^\alpha + \left( \frac{1}{2} \lambda - 2 \right) t^\alpha \right) \right) \right]. \quad (57)$$

$$u_{10}(x, t) = \frac{1}{2} \lambda \left[ 1 + \coth \left( \frac{1}{2\alpha} \lambda (x^\alpha + (1 - \lambda)t^\alpha) \right) \right]. \quad (58)$$

$$u_{11}(x, t) = \frac{1}{2} \left[ (\lambda + 1) + (\lambda - 1) \coth \left( -\frac{1}{4\alpha} (\lambda - 1) \left( x^\alpha + \frac{1}{2} (\lambda + 1) t^\alpha \right) \right) \right]. \quad (59)$$

$$u_{12}(x, t) = \frac{1}{2} \left[ (\lambda + 1) - (\lambda + 1) \coth \left( -\frac{1}{2\alpha} (\lambda - 1) (x^\alpha - (\lambda + 1) t^\alpha) \right) \right]. \quad (60)$$

Furthermore, equations (37) through (48) provide sets of traveling wave solutions:

$$u_{13}(x, t) = \begin{cases} \frac{1}{2} \left[ 1 - \frac{1}{2} \tanh \left( \frac{1}{8\alpha} \left( x^\alpha + \left( \frac{1}{2} - 2\lambda \right) t^\alpha \right) \right) \right. \\ \left. - \frac{1}{2} \coth \left( \frac{1}{8\alpha} \left( x^\alpha + \left( \frac{1}{2} - 2\lambda \right) t^\alpha \right) \right) \right] \end{cases}. \quad (61)$$

$$u_{14}(x, t) = \begin{cases} \frac{1}{2} \left[ 1 + \frac{1}{2} \tanh \left( \frac{1}{4\alpha} \left( x^\alpha + (\lambda - 1) t^\alpha \right) \right) \right. \\ \left. + \frac{1}{2} \coth \left( \frac{1}{4\alpha} \left( x^\alpha + (\lambda - 1) t^\alpha \right) \right) \right] \end{cases}. \quad (62)$$

$$u_{15}(x, t) = \begin{cases} \frac{1}{2} \lambda \left[ 1 - \frac{1}{2} \tanh \left( \frac{1}{8\alpha} \lambda \left( x^\alpha + \left( \frac{1}{2} \lambda - 2 \right) t^\alpha \right) \right) \right. \\ \left. - \frac{1}{2} \coth \left( \frac{1}{8\alpha} \lambda \left( x^\alpha + \frac{1}{2} \lambda - 2 \right) \right) \right] \end{cases}. \quad (63)$$

$$u_{16}(x, t) = \begin{cases} \frac{1}{2} \lambda \left[ 1 + \frac{1}{2} \tanh \left( \frac{1}{4\alpha} \lambda \left( x^\alpha + (1 - \lambda) t^\alpha \right) \right) \right. \\ \left. + \frac{1}{2} \coth \left( \frac{1}{4\alpha} \lambda \left( x^\alpha + (1 - \lambda) t^\alpha \right) \right) \right] \end{cases} \quad (64)$$

$$u_{17}(x, t) = \begin{cases} \frac{1}{2} \left[ (\lambda + 1) - \frac{1}{2} (\lambda - 1) \tanh \left( \frac{1}{8\alpha} (\lambda - 1) \left( x^\alpha + \frac{1}{2} (\lambda + 1) t^\alpha \right) \right) \right. \\ \left. - \frac{1}{2} (\lambda - 1) \coth \left( \frac{1}{8\alpha} (\lambda - 1) \left( x^\alpha + \frac{1}{2} (\lambda + 1) t^\alpha \right) \right) \right] \end{cases} \quad (65)$$

$$u_{18}(x, t) = \begin{cases} \frac{1}{2} \left[ (\lambda + 1) + \frac{1}{2} (\lambda - 1) \tanh \left( \frac{1}{4\alpha} (\lambda - 1) (x^\alpha - (\lambda + 1) t^\alpha) \right) \right. \\ \left. + \frac{1}{2} (\lambda - 1) \coth \left( \frac{1}{4\alpha} (\lambda - 1) (x^\alpha - (\lambda + 1) t^\alpha) \right) \right] \end{cases} \quad (66)$$

#### 4. Graphical depiction of the obtained solutions

Both 3D and 2D graphical visualizations are presented to illustrate the obtained solutions under various spatial ( $x$ ) and temporal intervals ( $t$ ), incorporating different values of the fractional order parameter,  $\alpha$ .

Figure 1 depicts 3D graphs that demonstrate the soliton solutions of  $u_1(x, t)$ , defined by a parameter within the interval  $[0, 2]$ , as shown in equation (49). The 3D graphs showcase exact solutions for  $\alpha = 1, 0.90, 0.80,$  and  $0.70$ , with the soliton solutions given in Figures (a-d), respectively. A 2D graph complements these visuals,

illustrating that an increase in  $\alpha$  results in a decrease in the magnitude of the soliton wave. Physically, this reflects the damping effect induced by higher fractional orders, where energy dissipates more effectively, leading to less pronounced wave amplitudes. The fractional order ( $\alpha$ ) significantly impacts wave behavior by governing the medium's dispersive and dissipative properties. Higher  $\alpha$  values lead to reduced energy localization and broader energy dispersion, resulting in diminished wave amplitudes. Unlikely, lower  $\alpha$  values enhance energy localization, creating sharper and more pronounced waveforms. This balance between energy conservation, dissipation, and dispersion highlights the critical role of fractional orders in shaping soliton dynamics, as evidenced by similar trends in nonlinear wave solutions across various parameter intervals.

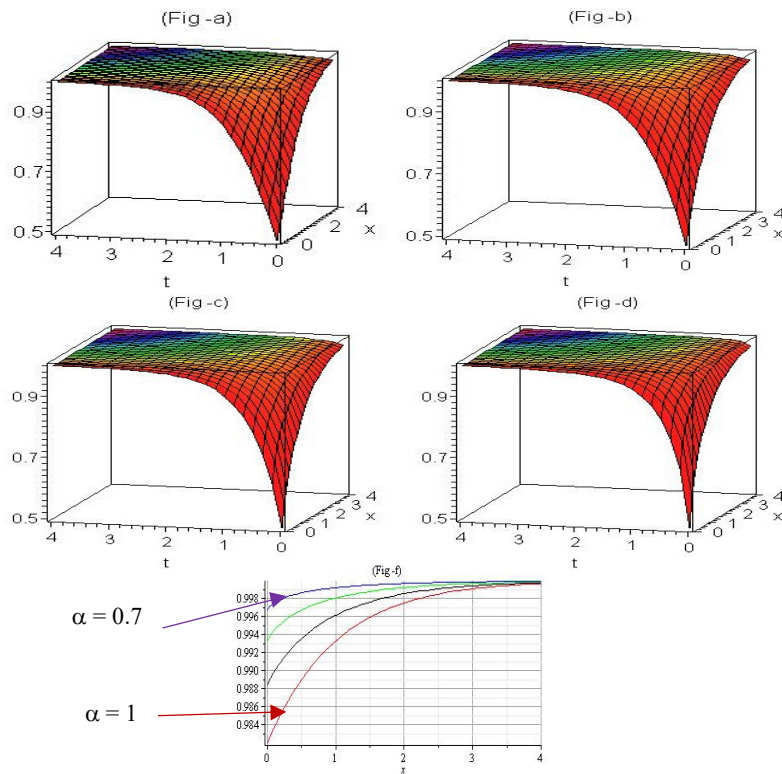


Fig. 1. 3D graphs of solutions  $u_1(x, t)$  for  $\lambda = 2$ , with  $0 \leq x, t \leq 4$ , and  $\alpha = 1, \alpha = 0.90, \alpha = 0.80, \alpha = 0.70$  in Figures (a), (b), (c), and (d), respectively. Figure (f) denotes the 2D plot with  $t = 2$

Figure 2 displays a detailed 3D depiction of the traveling wave solutions for  $u_7(x, t)$ , as presented in equation (55), to examine the dynamic behavior of nonlinear wave propagation. These solutions are acquired for a specific set of parameters over the interval  $[0, 2]$ , with  $\alpha = 1, 0.90, 0.80$ , and  $0.70$  corresponding to Figures (a-d), respectively. The graphs clearly illustrate that as  $\alpha$  decreases, the wavelength of

the traveling waves shortens, showing an inverse relationship between  $\alpha$  and the wavelength. This behavior reflects the increasing dispersion effects associated with lower fractional orders, where wave energy is more widely distributed, leading to reduced coherence and compactness in wave propagation. Additionally, the 2D graph (Figure f) reveals a reduction in wave magnitude as  $\alpha$  decreases from 1 to 0.70, signifying a damping effect. The fractional order affects both the spatial structure and energy concentration of waves, with lower  $\alpha$  values causing broader energy dispersion and damping. This has important applications in controlling wave propagation and minimizing energy concentration, as seen in material science and signal processing. Similar trends in other nonlinear systems highlight the significant role of fractional orders in wave dynamics.

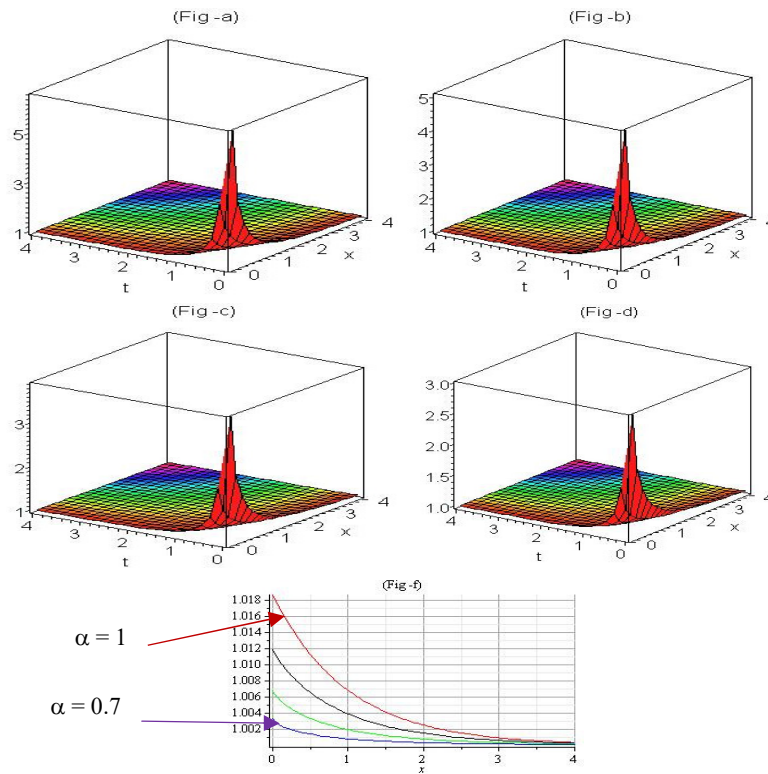


Fig. 2. 3D graph of solutions  $u_7(x, t)$  for  $\lambda = 2$  with  $0 \leq x, t \leq 4$ , and  $\alpha = 1$ ,  $\alpha = 0.90$ ,  $\alpha = 0.80$ ,  $\alpha = 0.70$  in Figures (a), (b), (c), (d) respectively. Figure (f) denotes the 2D plot with  $t = 2$

Figure 3 displays 3D graphical renderings of the solution  $u_{13}(x, t)$  under specific conditions, with both spatial and temporal variables ranging from 0 to 4. Figures (a-d) illustrate the behavior of  $u_{13}(x, t)$  for  $\alpha = 1, 0.90, 0.80$  and  $0.70$ , respectively. These depictions reveal the dynamic nature of traveling wave solutions arising from the nonlinear wave behavior given in equation (61). The 2D graph provides additional

insights, displaying that as  $\alpha$  increases from 0.70 to 1, the magnitude of  $u_{13}(x, t)$  becomes significantly larger. Higher fractional orders ( $\alpha$ ) enhance wave amplitude, reducing dissipation and increasing wave coherence, enabling stronger energy propagation over time and space. In contrast, lower fractional orders ( $\alpha$  close to 0.70) result in damped waves with reduced amplitude, reflecting greater dispersive and dissipative effects. These patterns highlight the crucial role of fractional order in shaping energy concentration and stability in traveling wave solutions, consistent across similar nonlinear wave systems.

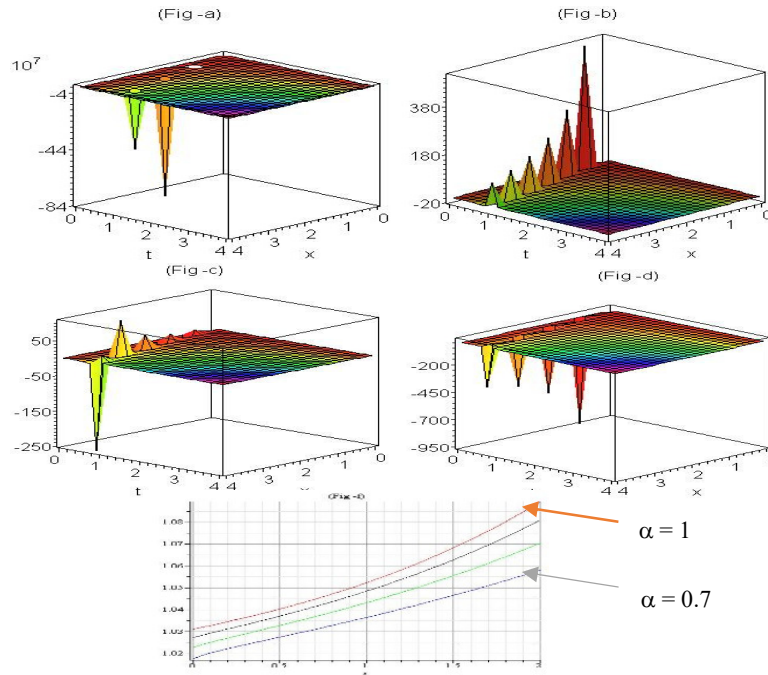


Fig. 3. 3D graph of solutions  $u_{13}(x, t)$  for  $\lambda = 2$  with  $0 \leq x, t \leq 4$  and  $\alpha = 1$ ,  $\alpha = 0.90$ ,  $\alpha = 0.80$ ,  $\alpha = 0.70$  in Figures (a), (b), (c), (d) respectively. Figure (e) denotes the 2D plot with  $t = 2$

## 5. Conclusion

This study applied the Tanh-Coth method to derive exact analytical solutions for the FBH equation using the CFD technique. A range of exact analytical solutions was obtained, emphasizing the influence of the fractional order on the outcomes. Solutions for various fractional orders were visually compared with the exact solutions in the classical scenario  $\alpha = 1$  illustrating the potential effect of different  $\alpha$  values on the solution characteristics. The physical attributes of the solutions were depicted using graphical representations. Compared to prior studies, the soliton solutions derived in this study are comparable to those provided by Wazwaz [13]

when  $\alpha$  equals 1. The results reveal that the Tanh-Coth method is efficient, simple, and reliable. The findings of this study serve as a valuable resource for future research in the context of wave phenomena. All calculations in this study were carried out using MAPLE. Future research could investigate the application of other analytical methods like the Homotopy Analysis Method (HAM) or Adomian Decomposition Method (ADM), to further expand the understanding and solution space of the FBH equation. In addition, exploring the influence of fractional parameters on further complex physical models or coupling the Tanh-Coth method with numerical simulations could give deeper insights. Finally, experimental validation of the acquired solutions and their application in real-world wave phenomena remain promising directions for prospective work.

## Acknowledgments

The authors extend their appreciation to the Deanship of Scientific Research at Northern Border University, Arar, KSA for funding this research work through the project number "NBU-FFR-2025-2877-04".

## References

- [1] Xiao, D., Fang, F., Pain, C.C., & Navon, I.M. (2017). A parameterized non-intrusive reduced order model and error analysis for general time-dependent nonlinear partial differential equations and its applications. *Computer Methods in Applied Mechanics and Engineering*, 317, 868-889. DOI: 10.1016/j.cma.2016.12.033.
- [2] Mohammed, A.A. (2017). An analytical method for space-time fractional nonlinear differential equations arising in plasma physics. *Journal of Ocean Engineering and Science*, 2(4), 288-292. DOI: 10.1016/j.joes.2017.09.002.
- [3] Lagergren, J.H., Nardini, J.T., Michael, L.G., Rutter, E.M., & Flores, K.B. (2020). Learning partial differential equations for biological transport models from noisy spatio-temporal data. *Proceedings of the Royal Society A*, 47620190800. DOI: 10.1098/rspa.2019.0800.
- [4] Xu, P., Long, F.-T., Shan, C., Li, G., Shi, F., & Wang, K.-J. (2024). The fractal modification of the Rosenau-Burgers equation and its fractal variational principle. *Fractals*, 32(06), P 2450121. DOI: 10.1142/S0218348X24501214.
- [5] Wang, K.-J., & Li, S. (2024). Study on the local fractional (3+1)-dimensional modified Zakharov-Kuznetsov equation by a simple approach. *Fractals*, 32(12), 2450091. DOI: 10.1142/S0218348X24500910
- [6] Wang, K.-J., Shi, F., Li, S., & Xu, P. (2024). The fractal Zakharov-Kuznetsov-Benjamin-Bona-Mahony equation: Generalized variational principle and the semi-domain solutions. *Fractals*, 32(12), 2450079. DOI: 10.1142/S0218348X24500797.
- [7] Jamil, A.H., Abdullah, M.S.A., & Mohamed, A.E. (2024). Exploring novel applications of stochastic differential equations: Unraveling dynamics in plasma physics with the Tanh-Coth method. *Results in Physics*, 60, 107684. DOI: 10.1016/j.rinp.2024.107684.
- [8] Kumar, M.U. (2022). Recent development of adomian decomposition method for ordinary and partial differential equations. *International Journal of Applied Computational Mathematics*, 8, 81. DOI: 10.1007/s40819-022-01285-6.

- [9] Muhammad, N., Fengquan, Li, & Hijaz, A. (2019). Modified Laplace variational iteration method for solving fourth-order parabolic partial differential equation with variable coefficients. *Computers and Mathematics with Applications*, 78, 2052-2062. DOI: 10.1016/j.camwa.2019.03.053.
- [10] Wang, K.J., Shi, F., Li, S., & Xu, P. (2024). Dynamics of resonant soliton, novel hybrid interaction, complex N-soliton and the abundant wave solutions to the (2+1)-dimensional Boussinesq equation. *Alexandria Engineering Journal*, 105, 485-495. DOI: 10.1016/j.aej.2024.08.015.
- [11] Benhammouda, B. (2016). A novel technique to solve nonlinear higher-index Hessenberg differential-algebraic equations by Adomian decomposition method. *SpringerPlus* 5, 590. DOI: 10.1186/s40064-016-2208-3.
- [12] Wazwaz, A.M. (2007). New solitary-wave special solutions with compact and noncompact structures for the Burgers-Huxley equation. *Applied Mathematics and Computation*, 184(2), 1002-1010.
- [13] Wazwaz, A.M. (2009). *Partial Differential Equations and Solitary Waves Theory*. Higher Education Press. Beijing and Springer-Verlag, Berlin.
- [14] Khalil, R., Al Horani, M., Yousef, A., & Sababheh, M. (2014). A new definition of fractional derivative. *Journal of Computational and Applied Mathematics*, 264, 65-70. DOI: 10.1016/j.cam.2014.01.002.
- [15] Malfliet, W. (1992). Solitary wave solutions of nonlinear wave equations. *American Journal of Physics*, 60(7), 650-654. DOI: 10.1119/1.17120.
- [16] Balcia, E. Ozturka, I., & Kartalb, S. (2019). Dynamical behaviour of fractional order tumor model with Caputo and conformable fractional derivative. *Chaos, Solitons and Fractals*, 123, 43-51. DOI: 10.1016/j.chaos.2019.03.032.
- [17] Zhao, D., & Luo, M. (2017). General conformable fractional derivative and its physical interpretation. *Calcolo*, 903-917. DOI: 10.1007/978-3-030-56962-4.
- [18] Eltayeb, A., Ahmed, M.A., Abaker, A., & Mohamed, I. (2021). Conformable fractional isothermal gas spheres. *New Astronomy*, 84, 101511. DOI: 10.1016/j.newast.2020.101511.
- [19] Morales-Delgado, V.F., Gómez-Aguilar, J.F., Escobar-Jiménez, R.F., & Taneco-Hernández, M.A. (2018). Fractional conformable derivatives of Liouville-Caputo type with low-fractionality. *Physica A.*, 503, 424-438. DOI: 10.1016/j.physa.2018.03.018.
- [20] Wazwaz, A.M. (2007). The tanh method for traveling wave solutions of nonlinear equations. *Applied Mathematics and Computation*, 190(2), 1797-1805.
- [21] El-Wakil, S.A., & Abdou, M.A. (2007). New exact travelling wave solutions using modified extended tanh-function method. *Chaos, Solitons & Fractals*, 31(4), 840-852.
- [22] Wazwaz, A.M. (2008). The tanh-coth and sine-cosine methods for reliable treatment of the Pochhammer-Chree equations. *Applied Mathematics and Computation*, 202(1), 333-342.
- [23] Bekir, A. (2008). Application of the tanh method to travelling wave solutions for non-linear equations. *Applied Mathematics and Computation*, 203(1), 133-143.
- [24] Asokan, R., & Vinodh, D. (2013). The tanh-coth method for soliton and exact solutions of the Sawada-Kotera equation. *International Journal of Pure and Applied Mathematics*, 117(13), 19-27.
- [25] Kaya, D. (2004). Exact solutions of nonlinear evolution equations by the generalized tanh-function method. *Physics Letters A*, 340(3-4), 183-188.
- [26] Wazwaz, A. (2004). The tanh method for traveling wave solutions of nonlinear equations. *Applied Mathematics and Computation*, 154, (3), 713-723.